



HAL
open science

Handheld laser-induced breakdown spectroscopy (LIBS) as a fast and easy method to trace gold

Anthony Pochon, Anne-Marie Desaulty, Laurent Bailly

► To cite this version:

Anthony Pochon, Anne-Marie Desaulty, Laurent Bailly. Handheld laser-induced breakdown spectroscopy (LIBS) as a fast and easy method to trace gold. *Journal of Analytical Atomic Spectrometry*, 2020, 35 (2), pp.254-264. 10.1039/c9ja00437h . hal-02911800

HAL Id: hal-02911800

<https://brgm.hal.science/hal-02911800v1>

Submitted on 9 Oct 2024

HAL is a multi-disciplinary open access archive for the deposit and dissemination of scientific research documents, whether they are published or not. The documents may come from teaching and research institutions in France or abroad, or from public or private research centers.

L'archive ouverte pluridisciplinaire **HAL**, est destinée au dépôt et à la diffusion de documents scientifiques de niveau recherche, publiés ou non, émanant des établissements d'enseignement et de recherche français ou étrangers, des laboratoires publics ou privés.



Distributed under a Creative Commons Attribution - NonCommercial 4.0 International License

Handheld Laser-Induced Breakdown Spectroscopy (LIBS) as a fast and easy method to trace gold

Anthony Pochon* (pochon.anthony@gmail.com), Anne-Marie Desaulty (am.desaulty@brgm.fr),
Laurent Bailly (l.bailly@brgm.fr)

BRGM, F-45060, Orléans, France

* Corresponding author

Abstract

Gold is traded in virtually every country around the world. Consequently, tracing gold provenance is a difficult but necessary task to ensure a responsible supply chain from deposit to consumer. Measuring the silver content is often the first step in characterizing gold to retrace its origin. In this study, laser-induced breakdown spectroscopy (LIBS) using a handheld instrument was evaluated as a fast and easy method to analyse the silver content in natural gold. Six commercial gold alloys and natural gold from French Guiana were used. Our results demonstrate that a handheld LIBS is relevant to gold traceability and is simple to use in the field. The micron-scale focused laser beam allows *in-situ* analyses of small gold grains with acceptable reproducibility. Univariate and multivariate regression modelling was performed to assess the best calibration model for quantification of the Ag content. The quadratic univariate model was selected for its good predictive ability, with a coefficient of determination R^2 of 0.99 and a mean average error of 0.36 wt.% Ag for prediction. The LIBS analyses of natural gold were compared to the EPMA data using a statistical test that allow distinct gold populations to be discriminated (or matched) and the results indicate it would be suitable for identifying unknown samples. We were able to successfully trace the origin of our “unknown” samples, a promising first step in the goal of delivering a low-cost field-based tool for responsible supply chain management.

Keywords: Laser induced breakdown spectroscopy, quantitative analysis, traceability, gold, silver content

48 1. Introduction

49 Gold is one of the most ancient and important metals worldwide. Considering its high
50 economic importance, the ability to identify the provenance of gold is fundamental in the minerals
51 industry. Traceability is particularly important for ensuring a responsible supply chain, especially in
52 the European Union given the recent emphasis on due diligence for minerals from conflict-affected
53 and high-risk areas (i.e. tin, tantalum, tungsten and gold) ^[1]. The best indicator mineral to trace
54 gold sources is gold itself ^[2] because it is a dense mineral, chemically stable and easily found in
55 the erosional products of gold systems (i.e. alluvial gold from placers). Indeed, drainage sediment
56 sampling, often the first step in a gold exploration strategy, is used to characterise alluvial gold
57 through its intrinsic features, such as its silver (Ag) content or its mineral inclusions, in order to
58 establish a link between a secondary (placer) deposit and its potential primary deposit ^[3-10].
59 Currently, the Ag content of a gold population is analysed with an electron probe micro analyser
60 (EPMA) and is generally displayed in cumulative percentile plots. This way of presenting the data
61 provides an easy and visually graphic comparison of the statistical distribution of the Ag content of
62 distinct gold populations and is helpful in understanding and constraining their origin ^[6, 9]. Whereas
63 the EPMA-based method is highly accurate and a proven method to characterize gold, the
64 approach is limited by both the cost of analyses and the time needed for laboratory preprocessing
65 (e.g. instrument calibration).

66 Hence, this study focusses on a fast and simple way to analyse the Ag content in natural
67 gold in a field laboratory with direct application for exploration and traceability. Laser-induced
68 breakdown spectroscopy (LIBS) was selected as the technology instead of X-Ray fluorescence
69 spectroscopy (XRF) principally because the newer handheld devices generally have a focused
70 laser beam less than 100 μm , whereas the analysed surface area (i.e. several mm) of a classical
71 handheld XRF system is much larger than most natural gold grains, except rare gold nuggets. The
72 LIBS method has already been applied to the accurate quantitative analysis of commercial gold
73 alloys and jewelry in order to determine their fineness ^[11-16]. Recently, Harmon *et al.* ^[17]
74 successfully used a handheld LIBS unit on natural gold nuggets from a museum collection to
75 classify and distinguish distinct populations of gold grains, most of which came from the USA, but

76 their analyses was not quantitative. Finally, the LIBS method has also been used in the field on
77 conflict-affected minerals (e.g. “coltan” ore ^[18]) and for the geochemical fingerprinting of
78 geomaterials ^[19-20].

79 To assess the performance of handheld LIBS instrumentation in determining Ag content in
80 gold grains, we analysed gold grains from five French Guiana gold populations. French Guiana
81 was chosen for a case study because it is currently explored for gold and constitutes a high-risk
82 area due to the presence of numerous illegal small-scale gold mines that represent a loss of
83 revenue for the government and cause widespread mercury pollution. In such a region, developing
84 an analytical method to determine the origin of gold to ensure its traceability has major health,
85 environmental and economic issues. A pilot study on gold from French Guiana led by BRGM and
86 WWF (World Wildlife Fund), has already developed a set of techniques for physicochemical
87 traceability of gold ^[21]. However, these techniques require extensive and time-consuming
88 laboratory preparation and analysis (e.g. EPMA, identification of mineral micro-inclusions, Pb-Ag-
89 Cu isotopic analyses). In this study, we propose that a handheld LIBS device can be used for rapid
90 *in situ* analysis of gold, thereby serving as a field-based decision-making tool for protecting human
91 health and the environment.

92

93 **2. Materials and methods**

94 **2.1 Standards and samples**

95 Six commercial gold alloys (18K5N, 18K4N, 18K3N, 18K2N, 18KPd13, 24K) from Cookson-
96 clal refinery (*i.e.* an affiliate of Heimerle + Meule GmbH) were used as standards for LIBS
97 calibration. The Ag content of these six commercial standards (*i.e.* according to the refiner) range
98 between 0.01 and 16 wt.%, comparable to the range of natural samples in French Guiana.

99 Natural gold grains used for this study consist of 13 samples coming from five alluvial gold
100 populations. The first one, Marc creek, were first studied by Augé *et al.* ^[21] as part of a project
101 funded by the WWF to test the analytical traceability of gold from French Guiana. Three samples of
102 gold grains were collected from this placer: the “B2”, “X2” and “A7” samples. Gold grains from the
103 others populations were provided by the official French Guiana refiner (SAAMP): the “33”, “39”,

104 “43” samples from the “Petit Inini” river; the “30”, “46”, “47” samples from the “Serpent” creek; the
105 “23”, “26”, “29” samples from the “Dimanche” creek and the “37” sample from the “Awa” creek.
106 Each sample of gold grains consists of about 20-40 individual grains between 0.05 and 3 mm in
107 size that were embedded in epoxy resin blocks and polished to expose grain cores. The dataset of
108 13 samples were divided in training and testing samples, following a classical ratio of about 3:1.
109 Among these 13 samples, four samples (“X2”, “43”, “46” and “29”) were randomly selected as
110 testing samples and considered as “unknown” samples and the nine remaining samples were used
111 for the characterisation of the five populations of gold grains. The analytical feasibility and
112 effectiveness of the LIBS method was thus tested by comparing the results obtained on the training
113 dataset to the four “unknown” samples. In addition, 10 individual gold grains from the “B2” sample
114 were selected and analysed without any preparation (“raw” gold grains) for comparison with the
115 polished gold grains. Standards and natural gold grains were analysed using Cameca SX-Five
116 electron probe micro-analyser (EPMA) at the ISTO-BRGM facilities (Orléans, France) (see details
117 in Table 1S, ESI). Five analyses for each standards and up to two analyses in the core of gold
118 grains were performed for Ag using a 20 kV accelerating voltage, a beam current of 40 nA and a
119 counting time of 30 s on peak. Whereas only the Ag content is of interest for our purpose, Au, Cu,
120 Hg and Pd were also analysed to obtain a full suite of elements concentrations in the standards.

121

122 **2.2 Instrumentation and measurement parameters**

123 The commercial SciAps © Z-200 C+ handheld LIBS analyser was used for this study. Its
124 portability and broad spectral range (i.e. 190-625 nm) make it a suitable tool to perform real-time
125 analyses in the field or measurements in a field laboratory^[17, 22]. The LIBS unit uses a 1064 nm
126 Nd:YAG pulsed laser with a 50 µm focused beam size to produce a plasma. This laser can deliver
127 energy pulses of 5-6 mJ per pulse with a 1-2 ns pulse duration and a repetition rate of 50 Hz. The
128 Z-200 C+ LIBS analyser displays multiple CCD based spectrometers covering a spectral range of
129 190–625 nm. The handheld unit can be operated in ambient atmosphere, but is also capable of
130 argon (Ar) purging that flows Ar directly to the focusing area on the sample surface at the location
131 of laser-induced plasma for signal enhancement (i.e. 10-fold increase in emission intensity ^[23]).

132 Each analysis was performed under constant argon flow with a pressure of around 10 psi.
133 Spectrometers are calibrated daily by ablating a piece of stainless steel inside the LIBS system in
134 order to correct possible spectral shifts. Because the LIBS system requires that the sample to be
135 held flush to the sampling window during acquisition and to prevent analytical bias, the LIBS unit
136 was anchored on a support with a xyz linear stage. For each standard, data acquisition consists of
137 11 single-shots for the calibration and 5-7 single-shots for the prediction. Each single-shot consists
138 of 8 cleaning (laser) pulses in order to ensure tape breakthrough, followed by the collection of 32
139 averaged spectra at the same location (Fig. 1a) in order to minimise the size of the affected
140 surface on the gold grains (because of their small size) and to avoid striking mineral inclusions.
141 Table 1 shows a summary of the acquisition parameters for the measure of the Ag content.

142

143 **2.3 Post-processing and statistical analysis of LIBS spectra**

144 SciAps Profile Builder software was used to initially process all data prior to exporting.
145 Microsoft Excel and its XLSTAT add-in were then used for additional data processing and for
146 statistical analysis. The three single-shot spectra for each standard were collected (*i.e.* 15 spectra)
147 by the LIBS units for the calibration of the Ag content. Before normalising the spectra, a polynomial
148 fitting of the baseline is applied followed by a baseline subtraction (Fig. 1b), which increases the
149 analytical performance^[24]. For the calibration, the emission line at 546.58 nm was selected for Ag
150 amongst the others possibilities (328.06, 338.31 and 520.92 nm) because it is the most intense
151 line. Following recommendations from others studies^[24-26] about the extraction method of raw LIBS
152 spectra, normalisation modes and calibration model validation, the following approach was used to
153 select the best calibration model:

- 154 (1) All the raw LIBS data were divided by the signal intensity of the Au emission line at
155 479.24 nm, representing the matrix-dominant element and the maximum signal
156 intensity. The 11 single-shots of the six standards were averaged later (Fig. 1b);
- 157 (2) Calibration models (Fig. 1c) were performed. The peak area of the emission line at
158 546.58 nm is extracted for univariate regressions (linear and quadratic) and multivariate
159 regressions (principal component (PCR) and partial least squares (PLSR) regressions)

160 were performed using a small portion of spectra comprised between 520 and 548 nm to
 161 overcome the overfitting;

162 (3) The validity and predictive ability of calibration models were assessed through an
 163 internal cross-validation test—the “classic” leave-one-out (LOO)—as well as an external
 164 prediction dataset. The external dataset consisting of 35 spectra thus corresponds to
 165 five LIBS single-shot spectra of the 24K and 18K5N standards, six LIBS single-shot
 166 spectra of the 18K4N, 18K3N and 18KPD13 standards and seven LIBS single-shot
 167 spectra of the 18K2N standard.

Table 1

Summary of acquisition parameters during Ag measurement using LIBS on gold grains

Number of locations	Standards: 11 single-shots for calibration and 5 or 6 for prediction Unknown samples: up to 3 single-shots
Cleaning shots per location	8
Data shots per location	32
Integration period	0
Integration delay	30
Argon flush (ms)	300
Test rate (Hz)	50
Clean rate (Hz)	50
Number of shots to average	32
Averaging method	Linear

168

169 For the goodness of fit and the predictive model assessment, the R^2 , LOO q^2 , root mean squared
 170 error (RMSE), and mean absolute error (MAE) were used and are respectively defined in Eqs. (1),
 171 (2), (3), and (4):

$$172 \quad R^2 = 1 - \frac{\sum_{i=1}^n (y_i - \hat{y}_i)}{\sum_{i=1}^n (y_i - \bar{y})} = 1 - \frac{\text{sum of squared residuals (SSR)}}{\text{total of sum of squares (TSS)}} \quad (1)$$

$$173 \quad LOO \ q^2 = \text{leave-one-out cross-validated } R^2 \quad (2)$$

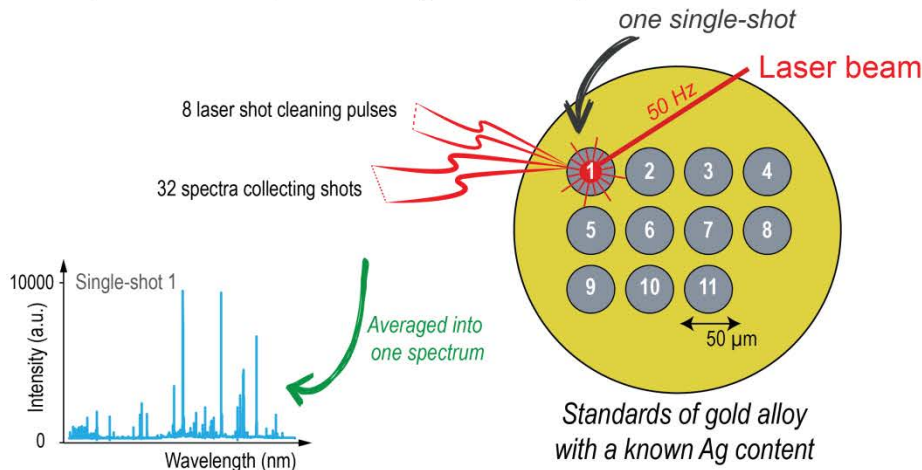
$$174 \quad RMSE = \sqrt{\frac{1}{n} \sum_{i=1}^n (y_i - \hat{y}_i)^2} \quad (3)$$

175 where RMSECV and RMSEP relate to the RMSE of cross-validation and prediction, respectively.

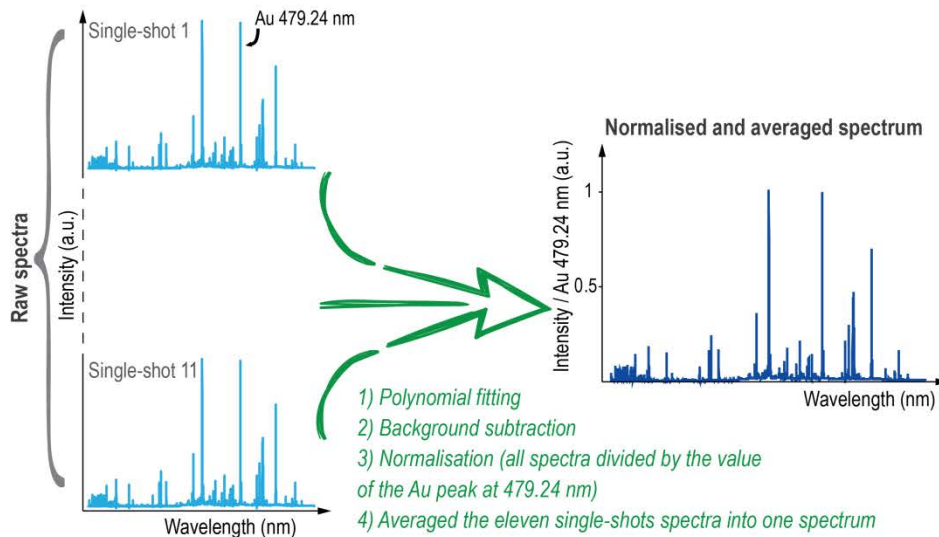
$$176 \quad MAE = \frac{\sum_{i=1}^n |\hat{y}_i - y_i|}{n} \quad (4)$$

177 where MAECV and MAEP relate to the MAE of cross-validation and prediction, respectively.

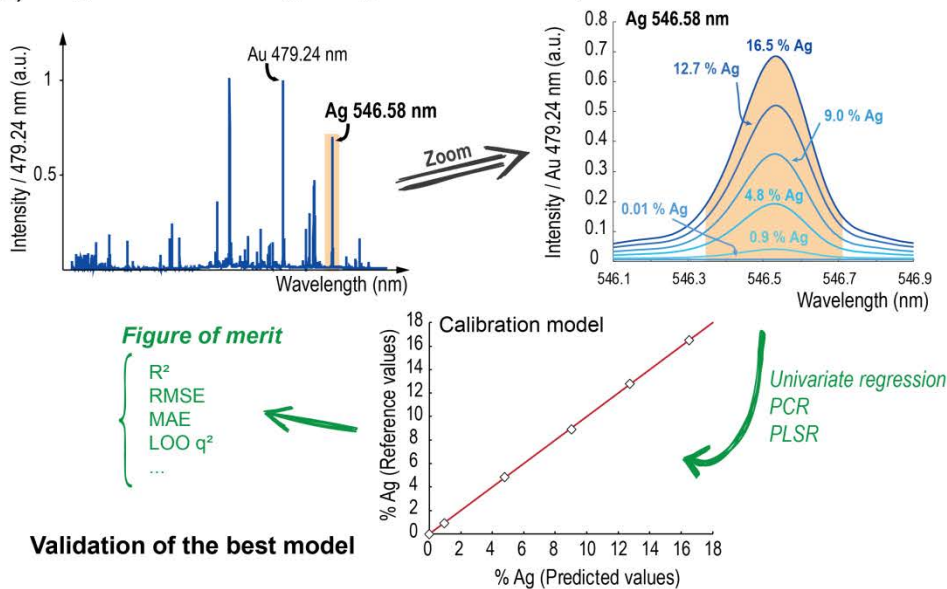
(a) Experimental setup of data acquisition for Ag calibration



(b) Post-processing of LIBS spectra



(c) Regression modelling for Ag calibration and quantification



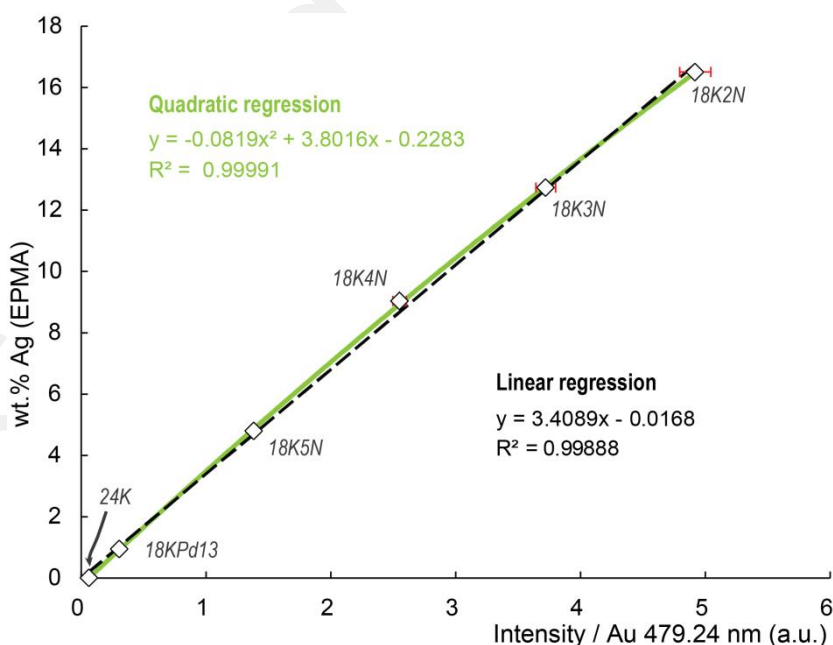
178

179 **Fig. 1** Schema illustrating the LIBS analysis approach used in this study. (a) Experimental setup used for Ag calibration on commercial
 180 gold alloys with the handheld LIBS tool. (b) Post-processing approach of LIBS spectra for calibration with the description of each step.
 181 (c) Regression modelling method for the Ag calibration.

182 3. LIBS approach for quantifying silver in alluvial gold

183 3.1 Regression modelling: univariate versus multivariate models

184 The analytical reproducibility of all measurements on the standards, given by the relative
185 standard error of the mean (SE) and the relative standard deviation (RSD), is largely satisfactory
186 with values of 2.5 % and 8.2 %, respectively (see details in Table 2S, ESI). For the conventional
187 univariate calibration (linear and quadratic), a simple ordinary least squares (OLS) regression
188 method was applied to calibration standards. Indeed, LIBS intensity is supposed to be a linear
189 function of the concentration of the chemical element of interest, even if curvatures can be
190 observed because of the self-absorption effects [27-28]. In our experiment, the relationship between
191 the Ag content and the intensity of the Ag emission line could be linear (Fig. 2) because of the
192 good superposition of the linear and quadratic curves. However, a comparison of the figures of
193 merit (Fig. 3a and Table 2) between the two univariate models displays difference of predictive
194 ability between them. A cross-validation test is rarely applied to an OLS regression, but the cross-
195 validation test were also performed on the univariate models for comparison with multivariate
196 models and to assess the best modelling.

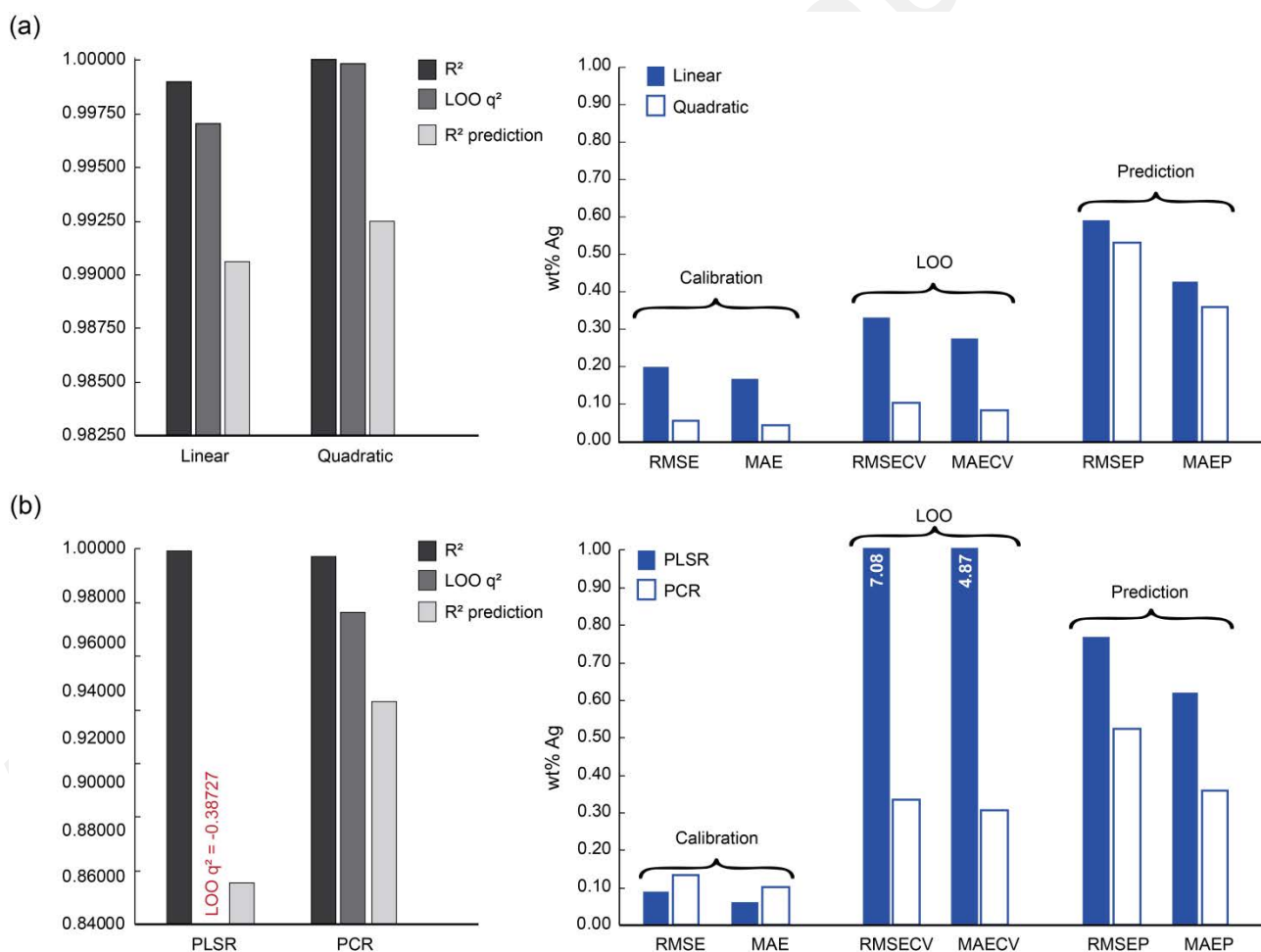


197

198 **Fig. 2** Linear and quadratic calibration curves using a classical OLS regression. The green line represents the quadratic
199 regression while the dashed line represents the linear one.

200

201 The quadratic model yields better results to the linear model with extremely low RMSE and
 202 MAE values of 0.05713 and 0.04453 wt.% Ag, respectively (0.20124 and 0.17110 wt.% Ag for the
 203 linear model). The coefficient of determination R^2 is also better for the quadratic regression with a
 204 value of 0.99991 compared to the value of 0.99888 for the linear regression (Fig. 3a and Table 2).
 205 The LOO q^2 is higher in the quadratic model than the linear one (0.99969 and 0.99693
 206 respectively), which indicates that the predictive power is more efficient for the quadratic
 207 regression. RMSECV and MAECV also show clearly that the quadratic model improve Ag
 208 calibration (Fig. 3a and Table 2). Finally, the quadratic model with the best RMSE and MAE of
 209 prediction (0.53320 and 0.36049 wt.% Ag, respectively) relative to linear model (*i.e.* 0.59573 wt.%
 210 Ag and 0.42835 wt.% Ag) is the best compromise to use as a univariate calibration model for
 211 quantifying Ag content in gold.



212

213 **Fig. 3** Figure of merit used to assess univariate (a) and multivariate (b) quantitative models. Coefficient of determination
 214 of the training calibration dataset (R^2) and of the prediction dataset (R^2 prediction) and the leave-one-out cross-validated
 215 (LOO) q^2 are displayed on the left. Root mean square error of calibration (RMSE), cross-validation (RMSECV) and
 216 prediction (RMSEP) and the mean absolute error of calibration (MAE), cross validation (MAECV) and prediction (MAEP)
 217 obtained for models displayed on the right.

218 For the multivariate calibration, the principal component regression (PCR) and the partial
 219 least square regression (PLSR) chemometric methods were used to quantify silver in gold. These
 220 methods are frequently used in LIBS quantification to overcome potential matrix effects in
 221 geological samples or to take into consideration the spectral interdependence between the lines of
 222 the considered elements and others elements ^[29]. Indeed, each line reflects varying degrees of
 223 information about the concentration of an element and potential correlations with others lines,
 224 increasing the number of independent variables and the complexity of the calibration. The PCR
 225 and the PLSR can extract relevant and hidden information in the LIBS spectra and then predict the
 226 concentration of the element of interest. PLSR is more complex than PCR because it takes into
 227 account all the variables (independent and dependent) and the signal noise. PLSR generally gives
 228 better results, although it has a general tendency of overfitting the training dataset.

Table 2

Results of the figures of merit obtained for univariate (linear and quadratic) and multivariate (PLSR and PCR) regression modelling

		Univariate models		Multivariate models	
		Linear	Quadratic	PLSR	PCR
Calibration					
<i>(n = 66 spectra)</i>	R ²	0.99888	0.99991	0.99979	0.99952
	RMSE	0.20124	0.05713	0.08627	0.13114
	MAE (wt %)	0.17110	0.04453	0.06039	0.09968
LOO cross validation					
<i>(repeated 6 times)</i>	LOO q^2	0.99693	0.99969	-0.38727	0.99693
	RMSECV	0.33335	0.10538	7.08045	0.33332
	MAECV (wt %)	0.27631	0.08767	4.87009	0.30601
Prediction					
<i>(n = 35 spectra)</i>	R ²	0.99055	0.99243	0.98442	0.99280
	RMSEP	0.59573	0.53320	0.76487	0.51996
	MAEP (wt %)	0.42835	0.36049	0.61748	0.35509

229
 230 The coefficient of determination R² is high and associated with low RMSE and MAE for the
 231 PLSR (0.99979, 0.08627 wt.% Ag and 0.06039 wt.% Ag respectively) and the PCR (*i.e.* 0.99952,
 232 0.13114 wt.% Ag and 0.09968 wt.% Ag). However, the negative value of LOO q^2 and the large
 233 RMSECV and RMSEP (7.08045 wt.% Ag and 0.76487 wt.% Ag respectively) for the PLSR model
 234 compared to univariate models illustrate very well its poor predictive modelling ability (Fig. 3b and
 235 Table 2). At the opposite, the similar results of cross-validation and prediction for the PCR model
 236 compared to the univariate regressions, with a value of RMSECV of 0.33332 wt.% Ag and a value

237 of RMSEP of 0.51996 wt.% Ag, show that the PCR model has a good predictive power. However,
 238 the PCR model appears more sensitive to missing data compared to quadratic regression as
 239 highlighted by the slightly poorer cross-validation result (Fig. 3b and Table 2). In this study,
 240 multivariate models appear not more powerful in prediction than a simple univariate model, which
 241 is why we selected the quadratic univariate regression as the best calibration curve for quantifying
 242 the Ag content in alluvial gold.

Table 3

Summary of descriptive statistics of the Ag content of the French Guiana gold samples

EPMA						LIBS					
	Descriptive statistics						Descriptive statistics				
	Min	Max	Median	Mean	Std		Min	Max	Median	Mean	Std
“Marc” creek ^[21]											
B2 (n=16)	3.60	11.85	5.08	6.09	2.72	(n=56)	1.08	13.09	4.57	4.82	3.69
B2 “raw” (n=12)							0.27	3.90	1.39	1.62	1.08
X2 ¹ (n=18)	2.57	11.14	4.41	5.21	2.56	(n=32)	2.14	12.78	5.17	5.83	2.92
A7 (n=15)	1.96	22.60	5.89	7.46	5.74	(n=15)	1.45	12.72	4.76	5.32	2.46
“Petit Inini” river											
SP33 (n=20)	6.27	19.05	8.17	8.88	2.81	(n=22)	2.46	13.33	7.43	7.51	2.26
SP39 (n=20)	2.58	12.55	7.24	7.51	2.25	(n=20)	2.25	12.12	7.07	7.24	2.17
SP43 ¹ (n=19)	6.08	12.37	7.55	7.92	1.76	(n=24)	6.06	13.91	7.77	7.98	1.61
“Serpent” creek											
SP30 (n=18)	1.10	2.37	1.66	1.71	0.35	(n=26)	0.34	3.16	1.55	1.60	0.65
SP46 ¹ (n=21)	1.22	6.92	1.84	2.33	1.55	(n=21)	1.01	2.87	1.40	1.61	0.54
SP47 (n=21)	1.23	2.67	1.69	1.80	0.39	(n=27)	1.10	2.79	1.63	1.71	0.46
“Dimanche” creek											
SP23 (n=26)	1.88	8.51	2.83	3.50	1.66	(n=24)	1.41	6.36	2.51	3.02	1.33
SP26 (n=22)	0.95	7.64	3.23	3.24	1.56	(n=25)	0.87	7.24	3.34	3.25	1.73
SP29 ¹ (n=29)	1.02	7.58	3.53	3.58	1.32	(n=22)	0.87	7.22	3.21	3.04	1.44
“Awa” creek											
SP37 (n=21)	5.17	16.77	6.76	7.76	2.84	(n=21)	4.78	8.09	6.61	6.64	0.86

¹ testing samples considered as “unknown” samples during this study in order to validate the methodology of traceability

243

244 3.2 Quantifying silver in alluvial gold

245 The LIBS analysis on alluvial gold grains was conducted in the same operating conditions
 246 as the gold alloy standards used in the calibration step (Table 1). The single-shot was performed
 247 on the core of each gold grain and the number of single-shots by grain depended on the grain size
 248 (e.g. only one single-shot for a small grain and up to three single-shots for larger grains). The
 249 depth of the laser ablation hole is about 4 μm, leading to a mass loss of about ~ 150 ng of gold and

250 making the LIBS technique barely destructive. The previously selected quadratic univariate
251 regression was then applied to quantify the Ag content in alluvial gold grains (see previous
252 section). Analyses of the Ag content obtained by the EPMA and LIBS methods are summarized in
253 Table 3 (complete analyses in Tables 3S and 4S, ESI, respectively). Note that gold grains
254 analysed with EPMA method are not necessarily the same as those analysed by the LIBS method.

255 The distribution of the Ag content of the different samples of gold grains, obtained by LIBS,
256 was compared to EPMA values using the non-parametric statistical test of Kolmogorov-Smirnov
257 (Table 4). This test, also called the K-S two samples test, compares the cumulative distribution
258 functions (CDFs) of two known samples ^[30-32]. It assesses the likelihood that two samples have the
259 same distribution (*i.e.* the “null” hypothesis). The K-S test calculates the maximum distance D
260 between two empirical CDFs. The more D increases, the more the distribution is different, meaning
261 that they are two distinct populations. If the distance D is lower than the critical distance D_{critical} and
262 the p -value (*i.e.* value of probability) is higher than the level of significance α , then the “null”
263 hypothesis cannot be rejected and the two subpopulations are considered as originating from the
264 same population. The level of significance α of the statistical test used in this study is 0.05. This
265 commonly used value gives a confidence degree of $1 - \alpha$ (95 %). The critical distance is
266 dependent on sample size and the level of significance ^[31]. In addition to K-S results, the CDFs of
267 the Ag content (LIBS and EPMA) of each training sample (*i.e.* the nine samples used for the
268 characterisation of the five populations of gold grains) are displayed in the Figure 4. Only the
269 training samples are mentioned in the following subsections.

270 - “Marc” creek population: the Ag contents of the gold grains from “B2” and “A7” samples
271 share first-order similarities with those obtained by EPMA (Table 3 and Fig. 4a). Except
272 for the maximum values of “A7” sample, which largely differ, the descriptive statistics
273 are similar, as illustrated by the limited gap of the median Ag values (about 0.8 wt.% Ag
274 for EPMA and for LIBS). When the EPMA and LIBS analyses of the gold grains from
275 “B2” are compared (Fig. 4a), the K-S test shows that the two distributions are similar
276 with a distance D of 0.286 lower than the critical distance (0.386) and a p -value of 0.262
277 higher than the level of significance α (Table 4). The K-S test shows a similar result
278 between the EPMA and LIBS analyses of the “A7” sample with a distance D of 0.333

279 lower than the critical distance (0.497) and a p -value of 0.375 higher than the level of
 280 significance α . The strong similarities between the two analytical methods (see the
 281 close proximity between the CDFs displayed in the Fig. 4a) provide a validation of the
 282 accuracy of Ag analysis in gold by handheld LIBS and a comparison between EPMA
 283 and LIBS datasets.

Table 4

Kolmogorov-Smirnov tests for the Ag content between the EPMA and the LIBS values from the studied French Guiana gold samples

	D	D critical	p-value ¹
“Marc” creek			
B2 (LIBS) / B2 (EPMA)	0.286	0.386	0.262
A7 (LIBS) / A7 (EPMA)	0.333	0.497	0.375
B2 (LIBS) / A7 (LIBS)	0.315	0.395	0.190
B2 (LIBS) / B2 “raw” (LIBS)	0.798	0.433	< 0.0001
“Petit Inini” river			
33 (LIBS) / 33 (EPMA)	0.232	0.420	0.627
39 (LIBS) / 39 (EPMA)	0.100	0.430	1.000
33 (LIBS) / 39 (LIBS)	0.186	0.420	0.860
“Serpent” creek			
30 (LIBS) / 30 (EPMA)	0.252	0.417	0.508
47 (LIBS) / 47 (EPMA)	0.258	0.415	0.474
30 (LIBS) / 47 (LIBS)	0.234	0.394	0.530
“Dimanche” creek			
23 (LIBS) / 23 (EPMA)	0.199	0.385	0.708
26 (LIBS) / 26 (EPMA)	0.190	0.408	0.817
23 (LIBS) / 26 (LIBS)	0.268	0.389	0.341
“Awa” creek			
37 (LIBS) / 37 (EPMA)	0.238	0.420	0.591

¹ the level of significance is $\alpha = 0.05$.

284
 285 - “Petit Inini” river population: the Ag contents of the gold grains from “33” and “39”
 286 samples appear very similar to that obtained by EPMA and between them (Table 3 and
 287 Fig. 4b). Except for EPMA extremum values of “33” sample, the descriptive statistics are
 288 extremely close, as illustrated by the slight difference between the median Ag values
 289 and the mean values (0.19 wt.% Ag and 0.27 wt.% Ag, respectively). The CDFs and the
 290 K-S tests between the two samples (LIBS and EPMA analyses) clearly shows that their

291 distributions are almost identical. The best example is illustrated by the comparison
292 between EPMA and LIBS values of “39” sample with a distance D of 0.100 lower than
293 the critical distance (0.430) and a maximum p -value of 1 (Table 4), and by the
294 superposition of the two CDFs (Fig. 4b).

295 - “Serpent” creek population: such as the preceding gold populations, the Ag contents of
296 the gold grains from “30” and “47” samples share several similarities between them and
297 with those obtained by EPMA (Table 3 and Fig. 4c). The median and the mean values
298 are very close and relatively low (~ 1.6 wt. % Ag and ~ 1.7 wt. % Ag, respectively). The
299 Ag content of the “Serpent creek” population varies very little only with a standard
300 deviation of 0.46, that is also well illustrated by the tight CDFs (Fig. 4c). The K-S tests
301 also show that the distributions between LIBS and EPMA data are very similar with a p -
302 value of 0.508 for the “30” sample and 0.474 for the “47” sample (Table 4). Result is
303 identical when comparing “30” and “47” samples with a distance D of 0.234 lower than
304 the critical distance (0.394) and a p -value of 0.530 higher than the level of significance
305 α .

306 - “Dimanche” creek population: as shown in Table 3 and Figure 4d, the Ag content of the
307 gold grains from the “Dimanche creek” population (*i.e.* “23” and “26” samples) appears
308 comparable with those obtained by EPMA. The median and the mean values are close.
309 For example, the mean values of the “26” sample are 3.24 wt. % Ag for EPMA and 3.25
310 wt. % Ag for LIBS, giving a difference of only 0.01. Unsurprisingly, the K-S tests gave a
311 result showing the close similarity between the CDFs (*e.g.* the p -value is 0.817 for the
312 “26” sample).

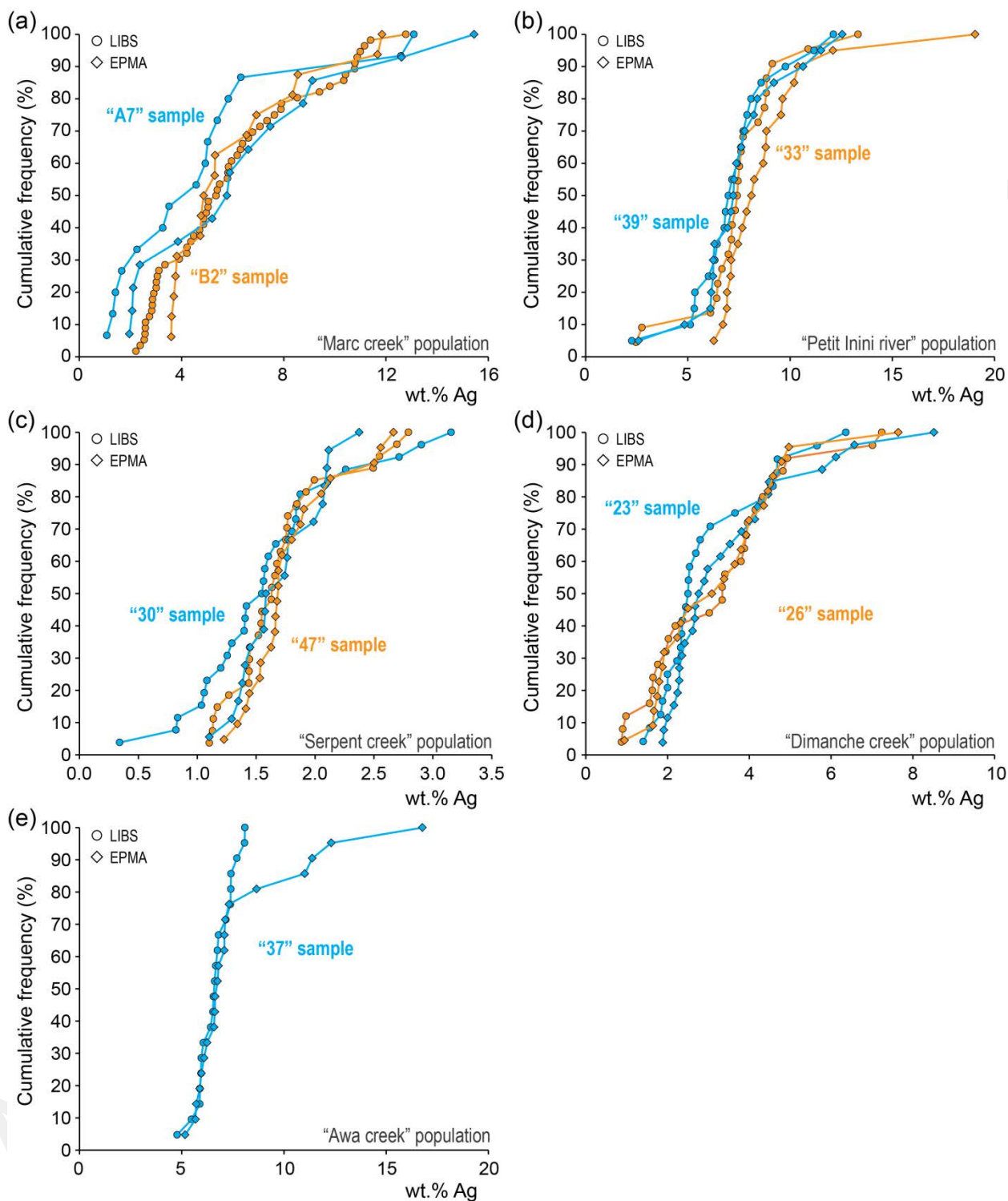
313 - “Awa” creek population: the Ag content of the gold grains from the “37” sample appears
314 very similar to that obtained by EPMA (Table 3 and Fig. 4e). Except for maximum
315 values, which largely differ, the descriptive statistics are relatively similar, as illustrated
316 by the limited gap of the median Ag values (only 0.15 wt.% Ag). Furthermore, the major
317 part of the CDFs is strictly superposed. The comparison between the EPMA and LIBS
318 analyses of the gold grains by the K-S statistics shows that the two distributions are

319

similar with a distance D of 0.238 lower than the critical distance (0.420) and a p -value

320

of 0.591 (Table 4).



321

322 **Fig. 4** Plots of cumulative distribution functions (CDFs) of the Ag content in alluvial gold grains. (a) Comparison between
323 the EPMA₂₁ and LIBS analyses of the “B2” and “A7” samples from the “Marc” creek population. (b) Comparison between
324 the EPMA and LIBS analyses of the “33” and “39” samples from the “Petit Inini” river population. (c) Comparison between
325 the EPMA and LIBS analyses of the “30” and “47” samples from the “Serpent” creek population. (d) Comparison between
326 the EPMA and LIBS analyses of the “23” and “26” samples from the “Dimanche” creek population. (e) Comparison
327 between the EPMA and LIBS analyses of the “37” sample from the “Awa” creek population.

328 Concerning the “raw” gold grains from “B2” sample (“Marc” creek population), the Ag
329 contents obtained by ablating the unpolished surface by LIBS are different when compared to the
330 polished gold grains (Table 3), and appear very low with a mean and median value about 3.2 times
331 lower than expected (Table 3). Furthermore, the K-S test indicate that the “raw” population is totally
332 different from the “polished” population (Table 4). The main causes of this difference could be
333 explained either by a poor laser-matrix interaction due to the surface roughness of a “raw” gold
334 grain and/or because the Ag content of the rim of an alluvial gold grain is typically depleted
335 compared to its core ^[21, 34-36]. This result implies that a minimum amount of sample preparation is
336 needed to expose the core of the grain in order to perform LIBS analysis on alluvial gold.

337

338 **4. Application to gold traceability**

339 **4.1 Discriminating distinct populations of gold**

340 A handheld LIBS could be used for analysing the silver content of gold during mineral
341 exploration in order to trace the primary sources of alluvial gold or for certifying the origin of gold
342 for traceability purposes (e.g. comparing the data to a database of French Guiana gold). In the
343 following subsections, the Ag content obtained by LIBS analyses are used to exhibit how an
344 handheld LIBS device might be useful to help discriminating distinct populations of gold grains and
345 tracing the golds grains origin. The nine training samples studied in the previous section have been
346 compiled into the five populations of gold from French Guiana with “B2” and “A7” samples forming
347 the “Marc” creek population, “33” and “39” samples forming the “Petit Inini” river population, “30”
348 and “47” samples forming the “Serpent” creek population, “23” and “26” samples forming the
349 “Dimanche” creek population and the “Awa” creek population which only consists of the “37”
350 sample (see the CDFs on the Fig. 5). These five populations of gold grains were compared
351 between them using the K-S test in order to check if we can discriminate distinct populations.
352 Results are displayed in the Table 5. The K-S tests clearly highlighted that the five populations are
353 statistically well distinct because the major part of results show a p -value lower than 0.0001, which
354 indicates that distributions are different with a confidence of 95 % (i.e. $1 - \alpha$). Consequently, in this

355 study, the distribution of the Ag content of these five populations of gold grains is significantly
 356 discriminant to be a key feature of a given population of gold.

Table 5

Comparison of the Ag content between the five French Guiana gold populations using the Kolmogorov-Smirnov test

	D	D critical	p-value ¹
"Marc" creek / "Petit Inini" river	0.523	0.265	< 0.0001
"Marc" creek / "Serpent" creek	0.798	0.254	< 0.0001
"Marc" creek / "Dimanche" creek	0.475	0.253	< 0.0001
"Marc" creek / "Awa" creek	0.539	0.338	0.0002
"Petit Inini" river / "Serpent" creek	0.929	0.287	< 0.0001
"Petit Inini" river / "Dimanche" creek	0.847	0.286	< 0.0001
"Petit Inini" river / "Awa" creek	0.452	0.363	0.006
"Serpent" creek / "Dimanche" creek	0.609	0.276	< 0.0001
"Serpent" creek / "Awa" creek	1.000	0.356	< 0.0001
"Dimanche" creek / "Awa" creek	0.878	0.355	< 0.0001

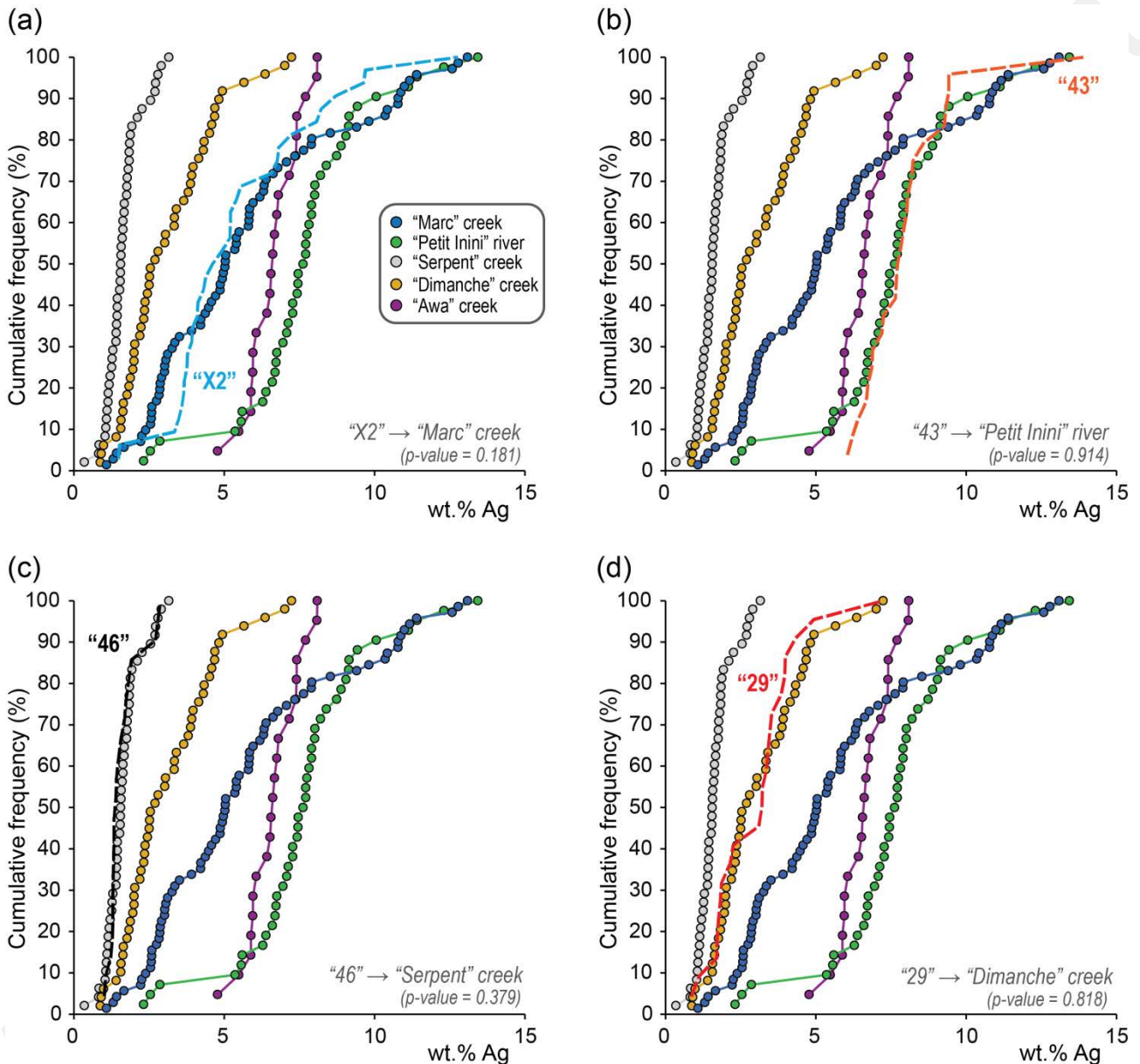
¹ the level of significance is $\alpha = 0.05$. "Marc" creek correspond to "B2" and "A7" samples, "Petit Inini" river correspond to "33" and "39" samples, "Serpent" creek correspond to "30" and "47" samples, "Dimanche" creek correspond to "23" and "26" samples, "Awa" creek only correspond to "37" sample

357

358 4.2 Tracing gold provenance

359 Because the previous subsection has demonstrated that the five population of gold studied
 360 were significantly distinct, this major feature can be used to match (or not) a potential "unknown"
 361 sample to a known populations of gold from a database (*i.e.* the nine samples in our study), a
 362 useful tool which could strongly help to retrace the provenance of gold. The CDFs of the Ag
 363 content obtained by LIBS for the five populations of gold and the four "unknown" samples set aside
 364 at the beginning of this study (*i.e.* the "X2", the "43", the "46" and the "29" samples) are displayed in
 365 the Figure 5. The CDF of the "X2" sample fits well with the CDF of the "Marc" creek population
 366 (Fig. 5a), suggesting that differences are not significant. Furthermore, the *p*-value (0.181), obtained
 367 from the K-S test on the LIBS analyses, indicates that the Ag contents follow a similar distribution
 368 function. The K-S tests between "X2" sample and others populations are displayed in the ESI
 369 (Table 5S) and show that "X2" only comes from the "Marc" creek population. Thereby, it can be
 370 statistically considered, with 95% confidence, as only one population of gold grains coming from
 371 the same location. The same reasoning can be applied to the three others "unknown" samples.
 372 The CDFs and results of the K-S tests (Table 5S, ESI) clearly demonstrate that the "43" sample fits

373 well with the “Petit Inini” river population (Fig. 5b), the “46” sample fits well with the “Serpent” creek
 374 population (Fig. 5c) and the “29” sample fits well with the “Dimanche” creek population (Fig. 5d).
 375 Thus, only with the distribution of the Ag content of gold grains, we are able to retrace the
 376 provenance of the four “unknown” samples among five populations of gold, making the handheld
 377 LIBS has a very useful tool for traceability purposes.



378
 379 **Fig. 5** Plots of cumulative distribution functions (CDFs) of the Ag content of the five gold grains populations from French
 380 Guiana and the four “unknown” samples split at the beginning of this study: the “X2” sample (a), the “43” sample (b), the
 381 “46” sample (c) and the “29” sample (d).
 382

383 4.3 Technical discussion

384 It should be noted, however, that a handheld LIBS is not a “magic” tool and has its limits.
 385 Our calibration has been only tested up to a content of 16 wt.% Ag, and further tests are needed

386 for gold grains with higher silver content. Furthermore, a large population database complicates
387 discrimination (or a matching) and should be coupled with other key elements (e.g. mineral micro-
388 inclusions, trace elements composition or isotopic analyses) as proposed by Chapman *et al.* ^[6] and
389 Augé *et al.* ^[21], which require more expensive and time-consuming techniques (e.g. EPMA, SEM)
390 relative to handheld LIBS. A critical point to take into consideration is the need of sample
391 preparation. Indeed, as for EPMA, the LIBS method requires a first step of polishing (see § 3.2).
392 However, whereas EPMA analyses require a fine polishing and a finishing with a very small
393 abrasive, which is achieved using diamond pastes of grades 1 µm and 0.25 µm, a coarse polishing
394 with silicon carbide disks is enough for analyses by handheld LIBS. Indeed, the only key point to
395 consider is to expose the grain core to the surface, a simple manual polishing of “raw” gold grain
396 could be enough to expose the core. Consequently, the time of sample preparation is considerably
397 reduced for LIBS relative to EPMA analyses. Furthermore, a handheld LIBS is easily transportable
398 and allows field investigations which is not the case of the EPMA. Thus, our results using a
399 handheld LIBS and the CDFs of the Ag content are very promising. This method could be a first
400 step in establishing gold traceability and opens a new realm of possibilities for supply chain
401 management.

402

403 **5. Concluding remarks**

404 The main motivation of this preliminary study was to investigate a technique that can rapidly
405 detect the Ag content in natural gold grains for tracing applications, thus reducing or avoiding more
406 costly sample preparation and processing requirements. A handheld LIBS unit was selected to
407 perform this test because it is compact and lightweight, making analysis an easy adaptation for a
408 field laboratory. The methodology developed in this study demonstrated the relevance and
409 usefulness of the LIBS technique. Univariate and multivariate models were developed from
410 commercial gold alloys for the calibration of the Ag content. The best calibration model is the
411 quadratic univariate model, providing an R^2 of 0.99991 and a good predictive power with RMSEP
412 of 0.53320 wt.% Ag and MAEP of 0.36049 wt.% Ag. This quadratic model is easy to use and
413 largely reduces the need for the classic but time-consuming multivariate model. The statistical

414 comparisons between the LIBS analyses of the five populations of gold (*i.e.* the nine training
415 samples) and the four “unknown” sample from French Guiana have shown that it is possible to
416 match two gold populations coming from the same location. Results have also shown that it is
417 possible to discriminate distinct populations, which would constitute a major advance in gold
418 traceability. The use of a handheld LIBS to trace the origin of gold from French Guiana gold
419 districts appears to have been successful and could be applied to other French Guiana gold
420 districts and other conflict-affected and high-risk areas afflicted by illegal mining, for example in
421 Democratic Republic of Congo within the Great Lakes region.

422

423 **Acknowledgements**

424 We are very grateful to Quantum RX to provide us the Sci Aps Z-200 C+ instrument and to the
425 SAAMP to provide us the major part of our gold samples from French Guiana. The authors thanks
426 Guillaume Wille for EPMA analyses, Cécile Fabre for her advice about the LIBS system and Marc
427 Dupayrat for its assistance with LIBS data. This work was supported by the CARNOT grant N° 17-
428 CARN-003-01. The editor H. Brewerton and two anonymous reviewers are thanked to help and
429 greatly improve the manuscript.

430

431 **References**

- 432 1 *OECD Due Diligence Guidance for Responsible Supply Chains of Minerals from Conflict-*
433 *Affected and High-Risk Areas*, OECD, 2016.
- 434 2 M. B. McClenaghan and L. J. Cabri, *Geochemistry Explor. Environ. Anal.*, 2011, **11**, 251–
435 263.
- 436 3 G. A. Desborough, R. H. Heidel, W. H. Raymond and J. Tripp, *Miner. Depos.*, 1971, **6**,
437 321–334.
- 438 4 J. C. Antweiler and W. L. Campbell, *Dev. Econ. Geol.*, 1977, **9**, 17–29.
- 439 5 R. C. Leake, R. J. Chapman, D. J. Bland, E. Condliffe and M. T. Styles, *Trans. Inst. Min.*
440 *Metall. (Section B Appl. Earth Sci.)*, 1997, **106**, B85-98.
- 441 6 R. J. Chapman, R. C. Leake and N. R. Moles, *J. Geochemical Explor.*, 2000, **71**, 241–268.
- 442 7 R. Chapman, B. Leake and M. Styles, *Gold Bull.*, 2002, **35**, 53–65.
- 443 8 R. J. Chapman and J. K. Mortensen, *J. Geochemical Explor.*, 2006, **91**, 1–26.
- 444 9 R. J. Chapman, M. M. Allan, J. K. Mortensen, T. M. Wrighton and M. R. Grimshaw, *Miner.*
445 *Depos.*, 2018, **53**, 815–834.
- 446 10N. R. Moles and R. J. Chapman, *Econ. Geol.*, 2019, **114**, 207–232.
- 447 11J. Amador-Hernández, L. E. García-Ayuso, J. M. Fernández-Romero and M. D. Luque de
448 Castro, *J. Anal. At. Spectrom.*, 2000, **15**, 587–593.
- 449 12L. García-Ayuso, J. Amador-Hernández, J. . Fernández-Romero and M. . Luque de Castro,
450 *Anal. Chim. Acta*, 2002, **457**, 247–256.
- 451 13A. Jurado-López and M. D. L. De Castro, *Appl. Spectrosc.*, 2003, **57**, 349–352.
- 452 14G. Galbács, N. Jedlinszki, G. Cseh, Z. Galbács and L. Túri, *Spectrochim. Acta Part B At.*
453 *Spectrosc.*, 2008, **63**, 591–597.
- 454 15S. Z. Shoursheini, B. Sajad and P. Parvin, *Opt. Lasers Eng.*, 2010, **48**, 89–95.
- 455 16N. Ahmed, R. Ahmed and M. A. Baig, *Plasma Chem. Plasma Process.*, 2018, **38**, 207–222.

- 456 17R. S. Harmon, R. R. Hark, C. S. Throckmorton, E. C. Rankey, M. A. Wise, A. M. Somers
457 and L. M. Collins, *Geostand. Geoanalytical Res.*, 2017, **41**, 563–584.
- 458 18R. S. Harmon, K. M. Shughrue, J. J. Remus, M. A. Wise, L. J. East and R. R. Hark, *Anal.*
459 *Bioanal. Chem.*, 2011, **400**, 3377–3382.
- 460 19R. S. Harmon, J. Remus, N. J. McMillan, C. McManus, L. Collins, J. L. Gottfried, F. C.
461 DeLucia and A. W. Miziolek, *Appl. Geochemistry*, 2009, **24**, 1125–1141.
- 462 20R. R. Hark and R. S. Harmon, Springer, Berlin, Heidelberg, 2014, pp. 309–348.
- 463 21T. Augé, L. Bailly, P. Bourbon, C. Guerrot, L. Viprey and P. Telouk, RP-64880-FR report,
464 BRGM, 2015, 147 p.
- 465 22B. Connors, A. Somers and D. Day, *Appl. Spectrosc.*, 2016, **70**, 810–815.
- 466 23Y. Iida, *Spectrochim. Acta Part B At. Spectrosc.*, 1990, **45**, 1353–1367.
- 467 24V. Motto-Ros, D. Syvilay, L. Bassel, E. Negre, F. Trichard, F. Pelascini, J. El Haddad, A.
468 Harhira, S. Moncayo, J. Picard, D. Devismes and B. Bousquet, *Spectrochim. Acta Part B*
469 *At. Spectrosc.*, 2018, **140**, 54–64.
- 470 25J. El Haddad, L. Canioni and B. Bousquet, *Spectrochim. Acta Part B At. Spectrosc.*, 2014,
471 **101**, 171–182.
- 472 26J. P. Castro and E. R. Pereira-Filho, *J. Anal. At. Spectrom.*, 2016, **31**, 2005–2014.
- 473 27J.-M. Mermet, *Spectrochim. Acta Part B At. Spectrosc.*, 2010, **65**, 509–523.
- 474 28D. W. Hahn and N. Omenetto, *Appl. Spectrosc.*, 2012, **66**, 347–419.
- 475 29T. Takahashi and B. Thornton, *Spectrochim. Acta Part B At. Spectrosc.*, 2017, **138**, 31–42.
- 476 30A. N. Kolmogorov, *G. Inst. Ital. Attuari*, 1933, **4**, 83–91.
- 477 31N. V. Smirnov, *Bull. Math. Univ. Moscou*, 1939, **2**, 3–14.
- 478 32F. J. Massey Jr, *J. Am. Stat. Assoc.*, 1951, **46**, 68–78.
- 479 33H. B. Mann and D. R. Whitney, *Ann. Math. Stat.*, 1947, pp. 50–60.
- 480 34G. A. Desborough, *Econ. Geol.*, 1970, **65**, 304–311.
- 481 35J. C. Groen, J. R. Craig and J. D. Rimstidt, *Can. Mineral.*, 1990, **28**, 207–228.

482 36J. B. Knight, J. K. Mortensen and S. R. Morison, *Econ. Geol.*, 1999, **94**, 649–664.

483

Accepted Manuscript